NASA TECHNICAL NOTE

NASA TN D-8258

ADAPTATION OF A GENERAL CIRCULATION MODEL TO OCEAN DYNAMICS

Richard E. Turner, Thomas H. Rees, and Gerard E. Woodbury

Langley Research Center
Hampton, Va. 23665

NATIONAL AERONAUTICS AND SPACE ADMINISTRATION • WASHINGTON, D. C. • OCTOBER 1976

1. Report No.	2. Government Accession No.	3. Recipient's Catalog No.
NASA TN D-8258		

4. Title and Subtitle	5. Report Date
ADAPTATION OF A GENERAL CIRCULATION MODEL TO OCEAN DYNAMICS	October 1976
	6. Performing Organization Code

7. Author(s)	8. Performing Organization Report No.
Richard E. Turner, Thomas H. Rees, and Gerard E. Woodbury	L-10756
	10. Work Unit No.
9. Performing Organization Name and Address	176-30-31-00
NASA Langley Research Center Hampton, VA 23665	11. Contract or Grant No.
	13. Type of Report and Period Covered
12. Sponsoring Agency Name and Address	Technical Note
National Aeronautics and Space Administration Washington, DC 20546	14. Sponsoring Agency Code

15. Supplementary Notes

Appendix A by Huw C. Davies, University of Reading, Berkshire, England.

16. Abstract

A new primitive-variable general circulation model of the ocean has been formulated in which fast external gravity waves are suppressed with rigid-lid surface constraint pressures which also provide a means for simulating the effects of large-scale free-surface topography. The surface pressure method is simpler to apply than the conventional stream function models, and the resulting model can be applied to both global ocean and limited region situations. Strengths and weaknesses of the model are also presented.

17. Key Words (Suggested by Author(s))	18. Distribution Statement
Ocean circulation Numerical modeling Hydrostatic flow Filtered primitive flow	Unclassified – Unlimited Subject Category 48

19. Security Classif. (of this report)	20. Security Classif. (of this page)	21. No. of Pages	22. Price*
Unclassified	Unclassified	38	$3.75

*For sale by the National Technical Information Service, Springfield, Virginia 22161

ADAPTATION OF A GENERAL CIRCULATION MODEL TO OCEAN DYNAMICS

Richard E. Turner, Thomas H. Rees,
and Gerard E. Woodbury
Langley Research Center

SUMMARY

A new primitive-variable general circulation model of the ocean has been developed in which fast external gravity waves may be suppressed with rigid-lid surface constraint pressures. The surface pressure filtering technique is easier to apply than the conventional stream function technique, and since the resulting model is derived in terms of primitive variables, it is conceptually simpler. From theoretical considerations, the model appears to be a candidate for limited region simulation, as well as simulation of global regions.

INTRODUCTION

Ocean circulation models are generally formulated either in terms of a stream function, such as the Bryan model given in reference 1, or else as a primitive-variable model, such as the one developed in reference 2. Both types of models have problems that one might like to avoid.

Stream function models are difficult to apply to multiconnected regions involving islands. Since the momentum equations are formulated in terms of a stream function, such models may be conceptually complex; and since stream function models simply cannot represent divergent flow fields, they are limited to large-scale problems where tidal motions can be neglected. (Tidal motions become more important in coastal zones and tidal basins.) Primitive-variable models, on the other hand, are conceptually simple and flexible. Islands and divergent flow fields are easily represented with primitive-variable ocean models. Unfortunately, primitive-variable models which do not filter fast external gravity waves associated with free-surface topography require large amounts of computer time.

The present model is a pseudo-primitive-variable model in which the fast external gravity waves are filtered by applying constraint pressures computed from the rigid-lid assumption. The resulting model can use a long time step and yet has the conceptual simplicity normally associated with a primitive-variable model. The model's vertical

structure is represented by a generally scaled variable that allows a simple but flexible treatment of bottom topography and land-sea boundaries as well as free-surface topography in situations where free-surface geometry is important. Islands are easily represented in the model because the boundary conditions at the islands are known a priori as opposed to stream function models wherein boundary values of the stream function around islands are difficult to obtain.

The surface pressure technique for filtering the external gravity wave is not entirely new. A similar approach is presented in reference 3; however, the present model has several advantages. First, the mathematical model presented herein allows a general stretching of the vertical coordinate rather than the linear stretching given in reference 3. Second, the model is derived in terms of spherical polar coordinates and is suitable for large-scale circulation problems. The rigid-lid model has been investigated analytically for open boundary situations and appears to be a candidate for such problems. Finally, the subgrid mixing formulation is presented in terms of a strain-rate tensor that properly vanishes when the fluid rotates in the rigid body mode. Consequently, erroneous shear stresses are not produced by simple rigid body rotations as in most previous works.

Thus, the present model fulfills a basic need that exists in the field of dynamic oceanography. A conceptually simple model has been established that can operate efficiently with a long time step. It is well suited to large-scale closed region simulation where free-surface topography is not important, as well as to small-scale open lateral boundary simulations where free-surface topography may be important.

NASA is presently studying potential use of satellites to monitor water pollution. Efforts will be made to determine the enhancement of remotely sensed data by use of circulation models. Since there is no way at the present time to penetrate the ocean depths by remote sensing, the initial attempt to study ocean pollution problems by remote sensing must be done by inferring subsurface phenomena from circulation models used in conjunction with remote and in situ measurements.

A description of the mathematical basis for the present model is given in reference 4. In the present report, the specialization of the mathematical model for ocean simulation is presented as well as preliminary computations on a 10° global grid. A simplified analysis of boundary condition specification for computation of rigid-lid constraint pressures is given in appendix A by Huw C. Davies. Detailed calculation for a model of the surface layers of the North Atlantic Ocean is presented and discussed in reference 5.

SYMBOLS

A	determinant of quasi-horizontal metric tensor in spherical polar coordinates; also, area in appendix A
B	parameter in equation of state
C_D	drag coefficient for bottom friction calculations
C_v	specific heat at constant volume of sea water
$D(x^\alpha,t)$	array specifying total depth distribution at horizontal position (x^1,x^2) and time t
D_f	flat-top depth distribution array or depth relative to the mean sea level geoid
E	internal energy per unit mass
F_α	group of terms in equations (24) and (25)
f	Coriolis parameter
g	acceleration due to gravity
g_{ij}	covariant element of the metric tensor
$H(x^j,t)$	four-dimensional function specifying instantaneous height of horizontal parametric surfaces referred to the mean sea level geoid
I,J,K	grid point indices
K_H	horizontal subgrid mixing coefficient
K_o	Von Kármán constant for turbulent flow, 0.4
K_V	vertical subgrid mixing coefficient
$\hat{L}_{ij}$	physical components of the deviatoric strain-rate tensor

$\hat{\ell}$	square root of second scalar for $\hat{\ell}^i_j$
$\hat{\ell}^i_j$	mixed tensor components of deviatoric strain-rate tensor
n_α	normal unit vector
P	pressure
$\tilde{P}$	approximate pressure
P_c	surface constraint pressure
P_f	hydrostatic pressure for rigid lid
q	perturbation constraint pressure in appendix A
r	mean radius of Earth
S	salinity mass fraction
$\hat{S}\left(\sqrt{A}\,\zeta\Phi\right)$	source term
S_j	physical velocity component of coordinate grid point in jth direction relative to rotating Earth
s	arc length
T	temperature, ^oC
t	time
U_j	physical component of fluid velocity vector relative to rotating Earth
$\tilde{U}_\alpha$	horizontal velocity component at end of first stage of integration
$U_\alpha\big\|_{x^3=0}$	horizontal velocity at ocean bottom
V_j	physical component of fluid velocity relative to coordinate grid points in jth direction

X^3	total depth of ocean in transformed coordinates
x^j	contravariant coordinate variables of reference coordinate system
z_j	Cartesian coordinates
Δ	grid increment
ϵ_α	horizontal perturbation velocity in appendix A
ζ	generalized density
λ	parameter in equation of state
ν	elemental fluid volume
ξ	function specifying layer thickness distribution
ρ	density of sea water
ρ_o	density of sea water at standard conditions
$\sigma_{\alpha\beta}$	elements of two-dimensional square matrix used to compute Coriolis force
τ	time increment
Φ	general physical parameter
ω	angular velocity of Earth
$\bar{\omega}$	mean molecular weight of sea water

Indices:

i,j	take on values 1, 2, or 3
t	computed at time t

α,β take on values 1 or 2 only

1,2,3 particular coordinate direction

The summation convention is used for multiple indices unless otherwise indicated.

Notation:

$\langle\ \rangle$ space and time average

$(\ )$ finite increment in $(\ )$

Primes denote the difference between instantaneous value and space-time average.

ANALYSIS

The model is based upon conservation of mass, momentum, salinity, and internal energy. The Navier-Stokes equations for a rotating, nearly spherical Earth are somewhat simplified by several important assumptions and approximations. First, the equation of motion for the vertical velocity is reduced to the hydrostatic approximation by neglecting local acceleration and other terms of the same magnitude. Second, the Boussinesq approximation, which neglects density differences except in the buoyancy term, is made. Third, since the equations are solved numerically on a finite-difference grid, stresses and processes occurring on scales too small to be resolved on the grid are parametrized or neglected. Molecular viscosity and conductivity are neglected. An empirical equation of state, giving density as a function of temperature, salinity, and pressure, is adopted. Finally, the "rigid-lid" approximation, which suppresses external inertia-gravitational oscillations by forcing the free surface to conform approximately to the mean sea level geoid, is optionally incorporated.

Coordinate System

For flexibility, the equations are formulated in spherical polar tensor notation. The coordinate system chosen for the ocean model is described in detail in reference 4. The coordinates are divided into two horizontal components x^1 and x^2 and one vertical component x^3. The bottom horizontal parametric surface $(x^3 = 0)$ follows the ocean bottom topography, while the upper coordinate surface $(x^3 = X^3)$ follows the upper surface of the ocean. Intermediate surfaces can be located as desired. To add flexibility to the model vertical structure, the equations of motion are formulated in terms of density multiplied by the vertical scale factor to form a "generalized density"

$$\zeta = \rho_o \sqrt{g_{33}} \qquad \left(\rho_o \approx 1\right) \tag{1}$$

The family of x^3-surfaces is controlled by the choice of $\sqrt{g_{33}}$, which can vary with x^1, x^2, x^3, and time. An x^3-surface is constructed by translating from $x^3 = 0$ a physical distance $\int_0^{x^3} \sqrt{g_{33}}\, dx^3$ perpendicular to the local x^3-surfaces.

The x^1 parametric lines at the surface $x^3 = 0$ are intersections of constant-longitude planes with the ocean bottom. The x^2 parametric lines at the surface $x^3 = 0$ are intersections of constant-latitude cones with the ocean bottom. Since the "horizontal" velocity components follow the x^1 and x^2 parametric lines, these components are generally not perpendicular to the local gravity vector. Therefore, in the momentum equations the components of gravity along the quasi-horizontal coordinate lines are included in the momentum balance. The validity of this formulation presupposes a small angle between dx^3 and the local gravity vector.

From reference 4, the square of the elemental arc length is shown to be approximately

$$(ds)^2 \approx \left(r\, dx^1\right)^2 + \left(r \sin x^1\, dx^2\right)^2 + g_{33}\left(dx^3\right)^2 \tag{2}$$

so that

$$g_{11} \approx (r)^2 \qquad g_{22} \approx \left(r \sin x^1\right)^2 \tag{3}$$

The determinant of the quasi-horizontal metric tensor is

$$A = g_{11} g_{22}$$

The unit vectors along dx^1, dx^2, and dx^3 form an orthogonal triad, and since g_{33} is allowed to vary with time, the grid points have physical velocities S_1, S_2, and S_3 relative to rotating Earth. The momentum equations are presented in terms of physical velocities U_1, U_2, and U_3 relative to rotating Earth such that

$$U_i = V_i + S_i$$

where V_i is the physical velocity of the fluid relative to the grid. All velocity components are given with respect to the local (dx^1,dx^2,dx^3) triad. In the model presented herein, S_1 and S_2 are always neglected as in reference 4, and S_3 is determined by the manner in which the vertical structure is chosen. The technique used to compute V_3 is presented in a subsequent section of this report.

Dynamic Equations

A rigorous derivation of the governing equations in spherical polar tensors is presented in reference 4. The equations are given here in final form only. The continuity equation in terms of the generalized density ζ is

$$\frac{\partial \zeta}{\partial t} + \frac{1}{\sqrt{A}} \frac{\partial}{\partial x^\alpha}\left(\sqrt{A}\,\zeta \frac{U_\alpha}{\sqrt{g_{\alpha\alpha}}}\right) + \frac{\partial}{\partial x^3}\left(\zeta \frac{V_3}{\sqrt{g_{33}}}\right) = 0 \tag{4}$$

where the second and third terms represent horizontal and vertical divergence, respectively.

The dynamic equation for momentum conservation in the x^1-direction (north-south direction) is

$$\begin{aligned}
&\frac{\partial}{\partial t}\left(\zeta U_1\right) + \frac{1}{\sqrt{A}} \frac{\partial}{\partial x^\alpha}\left(\sqrt{A}\,\zeta U_1 \frac{U_\alpha}{\sqrt{g_{\alpha\alpha}}}\right) + \frac{\partial}{\partial x^3}\left(\zeta U_1 \frac{V_3}{\sqrt{g_{33}}}\right) \\
&= -\frac{\sqrt{g_{33}}}{\sqrt{g_{11}}} \frac{\partial P}{\partial x^1} + 2\zeta\omega U_2 \cos x^1 - g\frac{\zeta}{\sqrt{g_{11}}} \frac{\partial H}{\partial x^1} - \frac{1}{\sqrt{A}} \frac{\partial}{\partial x^\alpha}\left(\sqrt{A}\,\zeta \frac{\langle U_1' U_\alpha' \rangle}{\sqrt{g_{\alpha\alpha}}}\right) \\
&- \frac{\partial}{\partial x^3}\left(\zeta \frac{\langle U_1' U_3' \rangle}{\sqrt{g_{33}}}\right) + \zeta\left(\frac{\langle U_2' U_2' \rangle}{\sqrt{g_{11}}} + \frac{U_2 U_2}{\sqrt{g_{11}}}\right) \cot x^1 + \frac{\zeta}{\sqrt{g_{11}}} U_3 \frac{\partial S_3}{\partial x^1}
\end{aligned} \tag{5}$$

In the above equation, the three terms on the left side (from left to right) represent accumulation and horizontal and vertical advection. The first term on the right side is the pressure gradient term. The second term on the right side is the Coriolis force term, where ω is the angular velocity of the Earth. The third term is the oblique gravity term which arises from departure of the quasi-horizontal parametric surfaces from the true

local horizontal. The instantaneous height of the horizontal coordinate surface referenced to the mean sea level geoid is

$$H\left(x^j,t\right) = \frac{1}{\rho_o}\int_0^{x^3} \zeta \, dx^3 - D_f$$

where D_f is the depth relative to the mean sea level geoid. The fourth and fifth terms on the right side of equation (5) represent horizontal and vertical subgrid diffusion, respectively. The brackets $\langle\ \rangle$ indicate space and time averaging, and the primed quantities indicate the difference between the instantaneous value and the space-time average. The next to last term represents centrifugal force, while the last term arises from motion of the vertical grid structure. Similarly, the momentum equation in the x^2-direction (east-west direction) is

$$\frac{\partial}{\partial t}\left(\zeta U_2\right) + \frac{1}{\sqrt{A}}\frac{\partial}{\partial x^\alpha}\left(\sqrt{A}\,\zeta U_2 \frac{U_\alpha}{\sqrt{g_{\alpha\alpha}}}\right) + \frac{\partial}{\partial x^3}\left(\zeta U_2 \frac{V_3}{\sqrt{g_{33}}}\right)$$

$$= -\frac{\sqrt{g_{33}}}{\sqrt{g_{22}}}\frac{\partial P}{\partial x^2} - 2\zeta\omega U_1 \cos x^1 - g\frac{\zeta}{\sqrt{g_{22}}}\frac{\partial H}{\partial x^2} - \frac{1}{\sqrt{A}}\frac{\partial}{\partial x^\alpha}\left(\sqrt{A}\,\zeta \frac{\langle U_2' U_\alpha'\rangle}{\sqrt{g_{\alpha\alpha}}}\right)$$

$$- \frac{\partial}{\partial x^3}\left(\zeta \frac{\langle U_2' U_3'\rangle}{\sqrt{g_{33}}}\right) - \zeta\left(\frac{\langle U_1' U_2'\rangle}{\sqrt{g_{11}}} + \frac{U_1 U_2}{\sqrt{g_{11}}}\right)\cot x^1 + \frac{\zeta}{\sqrt{g_{22}}} U_3 \frac{\partial S_3}{\partial x^2} \qquad (6)$$

The momentum equation in the x^3-direction is discarded in favor of the hydrostatic approximation.

The equation for conservation of salinity is

$$\frac{\partial}{\partial t}(\zeta S) + \frac{1}{\sqrt{A}}\frac{\partial}{\partial x^\alpha}\left(\sqrt{A}\,\zeta S \frac{U_\alpha}{\sqrt{g_{\alpha\alpha}}}\right) + \frac{\partial}{\partial x^3}\left(\zeta S \frac{V_3}{\sqrt{g_{33}}}\right)$$

$$= \frac{1}{\sqrt{A}}\hat{S}\left(\sqrt{A}\,\zeta S\right) - \frac{1}{\sqrt{A}}\frac{\partial}{\partial x^\alpha}\left(\sqrt{A}\,\zeta \frac{\langle S' U_\alpha'\rangle}{\sqrt{g_{\alpha\alpha}}}\right) - \frac{\partial}{\partial x^3}\left(\zeta \frac{\langle S' U_3'\rangle}{\sqrt{g_{33}}}\right) \qquad (7)$$

where the three terms on the left side represent accumulation and horizontal and vertical advection, and the second and third terms on the right side represent horizontal and vertical subgrid transport. The term $\frac{1}{\sqrt{A}}\hat{S}\left(\sqrt{A}\,\zeta S\right)$ is a source term. Similarly, the equation for conservation of internal energy E is

$$\frac{\partial}{\partial t}(\zeta E) + \frac{1}{\sqrt{A}}\frac{\partial}{\partial x^{\alpha}}\left(\sqrt{A}\,\zeta E\,\frac{U_{\alpha}}{\sqrt{g_{\alpha\alpha}}}\right) + \frac{\partial}{\partial x^{3}}\left(\zeta E\,\frac{V_3}{\sqrt{g_{33}}}\right)$$

$$= \frac{1}{\sqrt{A}}\hat{S}\left(\sqrt{A}\,\zeta E\right) - \frac{1}{\sqrt{A}}\frac{\partial}{\partial x^{\alpha}}\left(\sqrt{A}\,\zeta\,\frac{\langle E'U_{\alpha}'\rangle}{\sqrt{g_{\alpha\alpha}}}\right) - \frac{\partial}{\partial x^{3}}\left(\zeta\,\frac{\langle E'U_3'\rangle}{\sqrt{g_{33}}}\right) \tag{8}$$

where work of compression is ignored.

Density and Pressure Computations

Since the density of sea water is numerically very close to 1 g/cm^3, the Boussinesq approximation which neglects variations in ρ, except where multiplied by g, is a reasonable one and is used herein. This approximation simplifies the calculations. For example, the generalized density ζ is given simply by $\zeta = \sqrt{g_{33}}$. However, since the actual density is required in computing pressure, the technique for computing ρ is outlined in this section.

The empirical equation of state from reference 1 which gives density ρ (in g/cm^3) as a function of sea pressure P (in bars (1 bar = 0.1 MN/m^2)), salinity mass fraction S (in ppt), and temperature T (in $^{\circ}$C) is

$$\rho(S,T,P) = \frac{B}{1.000027(\lambda + 0.698B)} \tag{9}$$

where

$$B = P + 1 + 5890 + 38T - 0.375T^2 + 3S$$

and

$$\lambda = 1779.5 + 11.25T - 0.0745T^2 - (3.8 + 0.01T)S$$

Temperature T is given by

$$T = \frac{E\bar{\omega}}{C_v}$$

where C_v is specific heat at constant volume and $\bar{\omega}$ is mean molecular weight of sea water. The seas are assumed to be in hydrostatic equilibrium, so P is computed by integrating (with respect to x^3) the hydrostatic equation,

$$\frac{\partial P}{\partial x^3} = -g\rho\sqrt{g_{33}} \tag{10}$$

For given S and T, equations (9) and (10) form two simultaneous equations in two unknowns. To simplify the solution, an approximate pressure $\tilde{P}$ is first computed from equation (10) by setting $\rho = 1$ g/cm^3. The density is then taken as $\rho = \rho(S,T,\tilde{P})$ in equation (9), and equation (10) is again applied to give a closer approximation to P.

Vertical Velocity

In equations (4) to (8), V_3 is needed to compute vertical transport. The formulation allows $\sqrt{g_{33}}$ to be chosen quite generally provided that the following boundary conditions at the bottom and upper surfaces are met:

$$V_3 = 0 \quad \text{at} \quad x^3 = 0 \quad \text{and} \quad x^3 = X^3 \tag{11}$$

In the present model, V_3 (and hence S_3) is determined by requiring that

$$\zeta = D(x^\alpha,t)\ \xi(x^3)\rho_o \tag{12}$$

where the function D specifies the total depth distribution. The function $\xi(x^3)$ which defines the x^3 profile of the generalized density ζ is restricted so that

$$\int_0^{X^3} \xi(x^3)\, dx^3 = 1 \tag{13}$$

Otherwise, $\xi(x^3)$ can be any positive, single-valued function. Once this function is chosen, the expression for V_3 can be found by substituting equation (12) into equation (4), integrating with respect to x^3 from the bottom surface ($x^3 = 0$) to some specified x^3-surface, and applying the boundary conditions of equation (11). The result is

$$V_3 = -\frac{\sqrt{g_{33}}}{\zeta}\int_0^{x^3}\left[\rho_o\xi(x^3)\frac{\partial D}{\partial t} + \frac{1}{\sqrt{A}}\frac{\partial}{\partial x^\alpha}\left(\sqrt{A}\,\zeta\,\frac{U_\alpha}{\sqrt{g_{\alpha\alpha}}}\right)\right]dx^3 \tag{14}$$

An expression for $\partial D/\partial t$ can be obtained by evaluating equation (14) at $x^3 = X^3$ where $V_3 = 0$ (eq. (11)) and solving for $\partial D/\partial t$; that is,

$$\rho_o\frac{\partial D}{\partial t} = -\int_0^{X^3}\frac{1}{\sqrt{A}}\frac{\partial}{\partial x^\alpha}\left(\sqrt{A}\,\zeta\,\frac{U_\alpha}{\sqrt{g_{\alpha\alpha}}}\right)dx^3 \tag{15}$$

Equation (14) results directly from specifying ζ by equation (12). The determination of V_3 in this manner allows one to specify the x^3 grid point as a given fraction of the total depth regardless of the spatial variation of the depth. It should be pointed out that because of the formulation of the governing equations in terms of moving grid points, other methods of specifying V_3 could be adopted. For example, a hybrid Euler-Lagrange system of coordinates could be achieved by specifying $V_3 = 0$ along with $S_1 = S_2 = 0$.

Gravitational Instability

In the ocean, convective overturning maintains a stable vertical density profile. The hydrostatic approximation employed herein neglects vertical accelerations and prevents the model from simulating convective overturning. Therefore, a stable density profile must be maintained in the model artificially. Every water column is tested separately (at each integration step) for a gravitational instability. First, the reference-pressure densities are computed for each grid point in a given vertical column. If the grid values of reference-pressure densities decrease monotonically with grid distance from the bottom, then no gravitational instability exists in the given column. A gravitational instability is detected at level K (where K denotes the number of grid points from the bottom) when $\rho_{P_{surface}}(K) \leq \rho_{P_{surface}}(K+1)$. The instability is alleviated by mixing the two nodal cells to uniformity in temperature, salinity, and velocity. The new values of temperature, salinity, and velocity for both cells are computed to be

$$T(K) = T(K+1) = \frac{\zeta(K)\,T(K) + \zeta(K+1)\,T(K+1)}{\zeta(K) + \zeta(K+1)}$$

$$S(K) = S(K+1) = \frac{\zeta(K)\,S(K) + \zeta(K+1)\,S(K+1)}{\zeta(K) + \zeta(K+1)}$$

$$U_\alpha(K) = U_\alpha(K+1) = \frac{\zeta(K)\, U_\alpha(K) + \zeta(K+1)\, U_\alpha(K+1)}{\zeta(K) + \zeta(K+1)}$$

The total internal energy, salt, and momentum in the two cells are, therefore, conserved. The readjustment scheme given is chosen for simplicity and is intended to serve as an example only. A more complex and rigorous technique is given in reference 1.

Subgrid Mixing

The action of the unresolved subgrid waves on the resolvable waves is treated by a nonlinear kinematic eddy viscosity in the horizontal directions and by a specified viscosity in the vertical direction.

The subgrid velocity correlation tensor is taken to be proportional to the strain-rate tensor; that is, the velocity correlation components are related to the tensor strain-rate components by (from ref. 4)

$$\left\langle U_\alpha' U_\beta' \right\rangle = -K_H \hat{L}_{\alpha\beta} \qquad \left\langle U_\alpha' U_3' \right\rangle = -K_V \hat{L}_{\alpha 3}$$

where

$$\hat{L}_{ij} = \hat{\ell}^i{}_j \left(g_{ii}/g_{jj}\right)^{1/2} \qquad \text{(i and j not summed)} \qquad (16)$$

and the $\hat{\ell}^i{}_j$ are given for the quasi-two-dimensional case as

$$\hat{\ell}^1{}_1 = \left[\frac{\partial}{\partial x^1}\left(U_1 \sin x^1\right) - \frac{\partial U_2}{\partial x^2} - 2 \cos x^1 U_1\right] \Big/ \sqrt{g_{22}} \qquad (17a)$$

$$\hat{\ell}^1{}_2 = \sin x^1 \left[\frac{\partial U_1}{\partial x^2} + \frac{\partial}{\partial x^1}\left(U_2 \sin x^1\right) - 2 \cos x^1 U_2\right] \Big/ \sqrt{g_{22}} \qquad (17b)$$

$$\hat{\ell}^1{}_3 = \frac{\partial U_1}{\partial x^3} \Big/ \sqrt{g_{11}} \qquad (17c)$$

$$\hat{\ell}^2{}_1 = \hat{\ell}^1{}_2 \Big/ \left(\sin x^1\right)^2 \qquad (17d)$$

$$\hat{\ell}^2{}_2 = -\hat{\ell}^1{}_1 \tag{17e}$$

$$\hat{\ell}^2{}_3 = \frac{\partial U_2}{\partial x^3}\Big/\sqrt{g_{22}} \tag{17f}$$

$$\hat{\ell}^3{}_1 = \hat{\ell}^1{}_3\left(g_{11}/g_{33}\right) \tag{17g}$$

$$\hat{\ell}^3{}_2 = \hat{\ell}^2{}_3\left(g_{22}/g_{33}\right) \tag{17h}$$

$$\hat{\ell}^3{}_3 = 0 \tag{17i}$$

In the horizontal directions the strain-rate tensor is the basis for subgrid mixing. The strain-rate tensor, computed by assuming quasi-two-dimensional motion (zero strain rate in the vertical direction), is used to compute the horizontal kinematic eddy viscosity K_H. The tensor analogy for K_H, modeled after reference 6, is from reference 4,

$$K_H = \sqrt{2}\left(K_O \Delta\right)^2 \hat{\ell} \tag{18}$$

where $K_O = 0.4$, Δ is the reference grid dimension, and

$$\hat{\ell} = \left(\hat{\ell}^\alpha{}_\beta \hat{\ell}^\beta{}_\alpha\right)^{1/2} \tag{19}$$

In the vertical direction the subgrid mixing coefficient K_V is specified and may vary with depth.

The horizontal subgrid mixing for salinity and sensible heat flux from reference 4 are

$$\left\langle U_\alpha{}' S' \right\rangle = -K_H \frac{\partial S}{\partial x^\alpha}\Big/\sqrt{g_{\alpha\alpha}} \qquad (\alpha \text{ not summed}) \tag{20}$$

$$\left\langle U_\alpha{}' E' \right\rangle = -K_H \frac{\partial E}{\partial x^\alpha}\Big/\sqrt{g_{\alpha\alpha}} = -\frac{K_H}{\sqrt{g_{\alpha\alpha}}} \frac{C_v}{\bar{\omega}} \frac{\partial T}{\partial x^\alpha} \qquad (\alpha \text{ not summed}) \tag{21}$$

where C_v is the specific heat at constant volume and $\overline{\omega}$ is the mean molecular weight of sea water. The corresponding vertical subgrid mixing for salinity and sensible heat flux are

$$\left\langle U_3'S' \right\rangle = -K_V \frac{\partial S}{\partial x^3} \Big/ \sqrt{g_{33}} \tag{22}$$

$$\left\langle U_3'E' \right\rangle = -\frac{K_V}{\sqrt{g_{33}}} \frac{C_v}{\overline{\omega}} \frac{\partial T}{\partial x^3} \tag{23}$$

The approximation used herein is that K_V is identical for velocity, salinity, and temperature. If one desires, different values of K_H can be used.

Surface Pressure Approach to Rigid-Lid Approximation

For the present model a simple technique has been developed to filter external gravity waves. Incorporation of this filtering technique allows the model to simulate large-scale flow efficiently without troublesome external gravity waves. However, the model formulation allows deletion of the external gravity wave filter to simulate tidal motions and free-surface topography effects in small-scale studies. The gravity wave filter discussed in this section (which is a form of the rigid-lid approximation customarily used in stream function models of large-scale ocean circulation) is applicable both for problems having closed natural boundaries and for problems having open boundaries.

The technique is based upon the idea that fast external gravity waves can be filtered from the model by computing and applying the pressure that a rigid lid would exert on the ocean surface to negate time-dependent depth fluctuations. Application of the constraint pressure involves only the horizontal momentum equations.

The constraint pressure P_c is introduced into the momentum tendencies given in equations (5) and (6) by replacing P with $P_f + P_c$, where P_f is the hydrostatic pressure based upon the flat-top depth. By grouping terms, equations (5) and (6) can be rewritten as

$$\frac{\partial}{\partial t}\left(\zeta U_1\right) = -\frac{\sqrt{g_{33}}}{\sqrt{g_{11}}} \frac{\partial P_c}{\partial x^1} + \sqrt{g_{33}}\, F_1 \tag{24}$$

$$\frac{\partial}{\partial t}\left(\zeta U_2\right) = -\frac{\sqrt{g_{33}}}{\sqrt{g_{22}}} \frac{\partial P_c}{\partial x^2} + \sqrt{g_{33}}\, F_2 \tag{25}$$

where F_1 and F_2 contain all the remaining terms $\left(\text{divided by } \sqrt{g_{33}}\right)$ in equations (5) and (6). Equations (24) and (25) contain three unknowns, $\frac{\partial}{\partial t}\left(\zeta U_1\right)$, $\frac{\partial}{\partial t}\left(\zeta U_2\right)$, and P_c. The third equation needed to close the system can be obtained after noticing that P_c must be consistent with the requirement that the depth not vary with time. From equations (1), (12), and (13), the ocean depth given at a point $\left(x^1,x^2\right)$ is

$$D\left(x^\alpha,t\right) = \int_0^{X^3} \sqrt{g_{33}}\, dx^3 = \frac{1}{\rho_o} \int_0^{X^3} \zeta\, dx^3 \tag{26}$$

Thus, P_c must be consistent with

$$\rho_o \frac{\partial D}{\partial t} = \int_0^{X^3} \frac{\partial \zeta}{\partial t}\, dx^3 = 0 \tag{27}$$

Substituting equation (4) into equation (27), integrating, and applying the boundary conditions on V_3 (eq. (11)) result in

$$\rho_o \frac{\partial D}{\partial t} = -\frac{1}{\sqrt{A}} \frac{\partial}{\partial x^\alpha} \int_0^{X^3} \left(\sqrt{A}\,\zeta \frac{U_\alpha}{\sqrt{g_{\alpha\alpha}}}\right) dx^3 = 0 \tag{28}$$

When equations (24) and (25) are substituted into the derivative of equation (28) with respect to time and equation (26) is used, there follows

$$-\frac{1}{\sqrt{A}} \frac{\partial}{\partial x^\alpha} \frac{\sqrt{A}}{\sqrt{g_{\alpha\alpha}}} \int_0^{X^3} \frac{\partial}{\partial t}\left(\zeta U_\alpha\right) dx^3 = +\frac{1}{\sqrt{A}} \frac{\partial}{\partial x^\alpha}\left(\frac{\sqrt{A} D}{g_{\alpha\alpha}} \frac{\partial P_c}{\partial x^\alpha}\right) - \frac{1}{\sqrt{A}} \frac{\partial}{\partial x^\alpha} \int_0^{X^3} \frac{\sqrt{A}\sqrt{g_{33}}}{\sqrt{g_{\alpha\alpha}}} F_\alpha\, dx^3$$

which because of equation (27) vanishes leaving

$$\frac{1}{\sqrt{A}} \frac{\partial}{\partial x^\alpha}\left(\frac{\sqrt{A} D}{g_{\alpha\alpha}} \frac{\partial P_c}{\partial x^\alpha}\right) = \frac{1}{\sqrt{A}} \frac{\partial}{\partial x^\alpha} \frac{\sqrt{A}}{\sqrt{g_{\alpha\alpha}}} \int_0^{X^3} F_\alpha \sqrt{g_{33}}\, dx^3 \tag{29}$$

as the governing Poisson equation for P_c. Equation (29) is correct in theory; however, in practice P_c cannot be computed exactly and additional requirements are needed to insure that $\partial D/\partial t$ vanishes. These additional considerations are given in a subsequent section which deals with the numerical details.

Boundary Conditions

Boundary conditions to the dynamic equations are required at the ocean floor, along land-sea boundaries (and open boundaries, if any), and at the air-sea interface. Those boundary conditions which have not already been discussed are noted in this section.

Ocean bottom friction.- For currents in the bottom layer, friction terms are computed by use of a neutrally stable Prandtl layer model, originally used in an atmospheric circulation model (ref. 6). In essence, the Prandtl layer model assumes that vertical subgrid transport is in equilibrium within a thin bottom layer. The momentum transport in the Prandtl layer is derived from reference 6 as

$$\rho \left\langle U_3' U_\alpha' \right\rangle = -\rho C_D \left(U_\beta U_\beta \right)^{1/2} \left(U_\alpha - U_\alpha \Big|_{x^3=0} \right) \tag{30}$$

where $U_\alpha \Big|_{x^3=0} = 0$ and C_D is a drag coefficient.

Air-sea interface.- The interaction terms at the air-sea interface are wind stress $\rho \left\langle U_\alpha' U_3' \right\rangle$, heat transport rate $\rho \left\langle E' U_3' \right\rangle$, and salinity counterflux $\rho \left\langle S' U_3' \right\rangle$. The effect of evaporation upon the water mass of the system is neglected. These interaction terms must be specified. Methods for computing them are given in reference 6.

Land-sea boundaries.- The boundary condition at coastlines requires that mass transport normal to the beach be zero at the boundary. This condition is automatically satisfied by requiring the depth to be zero at boundary points. Thus, the coastline always follows a parametric line connecting boundary points.

When the rigid-lid approximation is used, an additional boundary condition – that the mass transport normal to the beach in a water column adjacent to a land boundary is zero – is required. This condition is imposed by subtracting the mean values of U_α throughout the column.

Open boundary conditions for rigid-lid applications.- A simplified analysis of boundary condition specification for the momentum equations and surface constraint pressure is given in appendix A. The approach is a version of a method by Davies in reference 7 for studying the uniqueness of solutions to the shallow water equations in a finite region. Along inflow boundaries, the velocity components U_α must be specified. The surface constraint pressure can be computed from an equation similar to equation (B11) in appendix B. Along outflow boundaries, either normal outflow velocity or else surface constraint pressure must be specified. When velocities are specified, they must satisfy mass conservation. Since P_c has an analogy with the surface topography caused by

external gravity waves, one might specify P_c by measuring the free-surface topography along the outflow boundaries. In many oceanographic flow situations, the geostrophic approximation in which the Coriolis force is balanced by the pressure gradient is justified. In the case of a limited region, it should be possible to choose boundaries through regions where the geostrophic approximation is valid. Then along an outflow boundary, approximate values for P_c would be computed from outflow velocities. To see this, recall equation (5) and retain only the pressure gradient, the oblique gravity term, and the Coriolis term. The sum of all three terms vanishes in the geostrophic approximation; thus, if dx^1 lies along the outflow boundary, one has the expression

$$-\frac{\sqrt{g_{33}}}{\sqrt{g_{11}}}\frac{\partial P}{\partial x^1} - \frac{g\zeta}{\sqrt{g_{11}}}\frac{\partial H}{\partial x^1} + 2\zeta\omega U_2 \cos x^1 \approx 0 \tag{31}$$

which can be integrated along the outflow boundaries to specify P_c.

COMPUTATIONAL SCHEME

The dynamic equations are solved over a three-dimensional grid by a finite-difference scheme which is similar to the method used in reference 6. The technique, central differencing in time and space, is often referred to as leapfrog.

Lattice Structure

The dependent variables are laid out over the three-dimensional lattice so that

$$\Phi\left(x^1,x^2,x^3\right) = \Phi\left(I\Delta x^1, J\Delta x^2, K\Delta x^3\right) = \Phi(I,J,K)$$

where the Δx^1 translation is from north to south, Δx^2 from west to east, and Δx^3 is along the local x^3 parametric line, perpendicular to the ocean bottom and positive up. On the two-dimensional horizontal grid, all dependent variables are defined at time $t - \tau$ on half of the grid points and at time t on the remaining grid points. The time structure does not change with x^3; in other words, at latitude index I and longitude index J, the variables are defined at the same time for each point in the column. Thus, the twin time lattices may be referred to as "even" or "odd," depending upon whether $I + J$ is even or odd. The even lattice, defined at time t, for example, is used to update the odd lattice from time $t - \tau$ to $t + \tau$. Then the odd lattice at $t + \tau$ is used to update the even lattice from time t to $t + 2\tau$.

Space Differencing of Dynamic Equations

To illustrate the computational sequence, integration of the salinity conservation equation is described. For simplicity put

$$\sqrt{A} = \sqrt{g_{\alpha\alpha}} = \sqrt{g_{33}} = \zeta = 1$$

with

$$\hat{S}\left(\sqrt{A}\,\zeta S\right) = 0$$

in equation (7) and get the simpler result

$$\frac{\partial S}{\partial t} = -\frac{\partial}{\partial x^{\alpha}}\left(SU_{\alpha}\right) - \frac{\partial}{\partial x^{3}}\left(SV_{3}\right) - \frac{\partial}{\partial x^{\alpha}}\left\langle S'U_{\alpha}'\right\rangle - \frac{\partial}{\partial x^{3}}\left\langle S'U_{3}'\right\rangle \tag{32}$$

The subgrid mixing given by equations (20) and (22) with the assumed simplifications becomes

$$\left\langle S'U_{\alpha}'\right\rangle = -K_{H}\frac{\partial S}{\partial x^{\alpha}} \qquad \left\langle S'U_{3}'\right\rangle = K_{V}\frac{\partial S}{\partial x^{3}} \tag{33}$$

The quantities V_3 and $\left\langle S'U_{3}'\right\rangle$ are computed at $(I,J,K\pm1/2)$, whereas the quantities $\left\langle S'U_{\alpha}'\right\rangle$ are computed at $(I\pm1/2,J,K)$ and $(I,J\pm1/2,K)$. Thus, to update dependent variables on the odd lattice from time $t - \tau$ to time $t + \tau$, one uses the following procedure:

(1) Use the even lattice at time t to compute

$$\frac{\partial}{\partial x^{\alpha}}\left(SU_{\alpha}\right) = \frac{S(I+1,J,K)\,U_{1}(I+1,J,K) - S(I-1,J,K)\,U_{1}(I-1,J,K)}{2\,\Delta x^{1}}$$

$$+\frac{S(I,J+1,K)\,U_{2}(I,J+1,K) - S(I,J-1,K)\,U_{2}(I,J-1,K)}{2\,\Delta x^{2}}$$

and

$$\frac{\partial}{\partial x^{3}}\left(SV_{3}\right) = \frac{S(I,J,K+1/2)\,V_{3}(I,J,K+1/2) - S(I,J,K-1/2)\,V_{3}(I,J,K-1/2)}{\Delta x^{3}}$$

where

$$S(I,J,K\pm1/2) = \frac{S(I+1,J,K\pm1) + S(I-1,J,K\pm1) + S(I,J+1,K\pm1) + S(I,J-1,K\pm1)}{8}$$

$$+ \frac{S(I+1,J,K) + S(I-1,J,K) + S(I,J+1,K) + S(I,J-1,K)}{8}$$

(2) Use the odd lattice at time $t - \tau$ to compute

$$\frac{\partial}{\partial x^3}\left\langle S' U_3' \right\rangle = -\frac{\partial}{\partial x^3}\left(K_V \frac{\partial S}{\partial x^3}\right)$$

$$= -\frac{K_V(K+1/2)}{\Delta x^3}\left[\frac{S(I,J,K+1) - S(I,J,K)}{\Delta x^3}\right] + \frac{K_V(K-1/2)}{\Delta x^3}\left[\frac{S(I,J,K) - S(I,J,K-1)}{\Delta x^3}\right]$$

Recall that K_V is specified at each vertical level.

(3) Use both the odd lattice at time $t - \tau$ and the even lattice at time t to compute

$$\frac{\partial}{\partial x^\alpha}\left\langle S' U_\alpha' \right\rangle = -\frac{\partial}{\partial x^\alpha}\left(K_H \frac{\partial S}{\partial x^\alpha}\right)$$

$$= -\frac{K_H(I+1/2,J,K)}{\Delta x^1}\left[\frac{S(I+1,J,K) - S(I,J,K)}{\Delta x^1}\right] + \frac{K_H(I-1/2,J,K)}{\Delta x^1}\left[\frac{S(I,J,K) - S(I-1,J,K)}{\Delta x^1}\right]$$

$$- \frac{K_H(I,J+1/2,K)}{\Delta x^2}\left[\frac{S(I,J+1,K) - S(I,J,K)}{\Delta x^2}\right] + \frac{K_H(I,J-1/2,K)}{\Delta x^2}\left[\frac{S(I,J,K) - S(I,J-1,K)}{\Delta x^2}\right]$$

where, for example, $K_H(I+1/2,J,K)$ is computed from equations (16) to (19). From equations (16) and (17), let

$$\hat{L}_{11} = -\hat{L}_{22} = \frac{U_1(I+1,J,K) - U_1(I,J,K)}{\Delta x^1} - \frac{A(U_2) - B(U_2)}{\Delta x^2}$$

where

$$A(U_2) = \frac{U_2(I+1,J,K) + U_2(I+1,J+1,K) + U_2(I,J+1,K) + U_2(I,J,K)}{4}$$

and

$$B(U_2) = \frac{U_2(I+1,J,K) + U_2(I+1,J-1,K) + U_2(I,J-1,K) + U_2(I,J,K)}{4}$$

Then

$$\hat{L}_{12} = \hat{L}_{21} = \frac{U_2(I+1,J,K) - U_2(I,J,K)}{\Delta x^1} + \frac{A(U_1) - B(U_1)}{\Delta x^2}$$

where $A(U_1)$ and $B(U_1)$ are defined in a manner similar to $A(U_2)$ and $B(U_2)$, respectively. Using equations (18) and (19), one gets

$$K_H(I+1/2,J,K) = 2(K_o)^2 \, \Delta x^1 \, \Delta x^2 \left[\left(\hat{L}_{11} \right)^2 + \left(\hat{L}_{12} \right)^2 \right]^{1/2}$$

The values of $K_H(I-1/2,J,K)$, $K_H(I,J+1/2,K)$, and $K_H(I,J-1/2,K)$ are computed by simple permutations of the indices. Note that $\hat{L}_{11}$ and $\hat{L}_{12}$ were simplified because of the assumption $\sqrt{A} = \sqrt{g_{\alpha\alpha}} = \sqrt{g_{33}} = 1$.

Time Differencing for Dynamic Equations and Constraint Pressure

Since the constraint pressure affects only the momentum tendencies, it is convenient to break the integration process into two distinct stages. In the first stage the dependent variables ζ, S, and E are updated with equations (4), (7), and (8), respectively. Since P_c is not known in the first stage, U_1 and U_2 are updated with $P_c = 0$ in equations (24) and (25). At the end of the first-stage integration, ζ, S, and E have the correct new values while U_1 and U_2 have incorrect values denoted by $\tilde{U}_1$ and $\tilde{U}_2$. For clarity, equations (24) and (25) may now be rewritten in terms of $\tilde{U}_1$ and $\tilde{U}_2$ by using

$$\frac{(\zeta U_1)^{t+\tau}}{2\tau} - \frac{(\zeta U_1)^{t-\tau}}{2\tau} \equiv \frac{(\zeta U_1)^{t+\tau} - \left(\zeta^{t+\tau}\tilde{U}_1\right)}{2\tau} + \frac{\left(\zeta^{t+\tau}\tilde{U}_1\right) - (\zeta U_1)^{t-\tau}}{2\tau} \qquad (34)$$

$$\frac{(\zeta U_2)^{t+\tau}}{2\tau} - \frac{(\zeta U_2)^{t-\tau}}{2\tau} \equiv \frac{(\zeta U_2)^{t+\tau} - \left(\zeta^{t+\tau}\tilde{U}_2\right)}{2\tau} + \frac{\left(\zeta^{t+\tau}\tilde{U}_2\right) - (\zeta U_2)^{t-\tau}}{2\tau} \tag{35}$$

The first-stage integration of the momentum equations is defined to be

$$\frac{\left(\zeta^{t+\tau}\tilde{U}_1\right) - (\zeta U_1)^{t-\tau}}{2\tau} = \sqrt{g_{33}}\, F_1 \tag{36}$$

and

$$\frac{\left(\zeta^{t+\tau}\tilde{U}_2\right) - (\zeta U_2)^{t-\tau}}{2\tau} = \sqrt{g_{33}}\, F_2 \tag{37}$$

In the second stage of integration, the correct values of U_1 and U_2 are found from the equations

$$\frac{(\zeta U_1)^{t+\tau} - \left(\zeta^{t+\tau}\tilde{U}_1\right)}{2\tau} = -\frac{\sqrt{g_{33}}}{\sqrt{g_{11}}} \frac{\partial P_c}{\partial x^1} \tag{38}$$

and

$$\frac{(\zeta U_2)^{t+\tau} - \left(\zeta^{t+\tau}\tilde{U}_2\right)}{2\tau} = -\frac{\sqrt{g_{33}}}{\sqrt{g_{22}}} \frac{\partial P_c}{\partial x^2} \tag{39}$$

In order to solve equations (38) and (39) for $U_1^{t+\tau}$ and $U_2^{t+\tau}$, a third equation for P_c is needed. In theory, one can substitute equations (38) and (39) into the time derivative of equation (28) and solve a Poisson-type equation for P_c at time $t + \tau$ as denoted in equation (29). Then $U_1^{t+\tau}$ and $U_2^{t+\tau}$ can be found from equations (38) and (39). The fallacy in this simplistic approach is that P_c cannot be found exactly; consequently, equation (27) would be violated over a long period of time. The proper approach, then, is to apply equation (28) in such a way that the time variation of $D(x^\alpha,t)$ is bounded. More specifically, equation (28) is replaced by its time-discretized counterpart evaluated at time $t + \tau$, so that

$$\left(\frac{\partial D}{\partial t}\right)^{t+\tau} = \frac{D^{t+2\tau} - D^{t}}{2\tau} = -\frac{1}{\sqrt{A}}\frac{\partial}{\partial x^{\alpha}}\left[\frac{\sqrt{A}}{\sqrt{g_{\alpha\alpha}}}\int_{0}^{X^3}\left(\zeta U_{\alpha}\right)^{t+\tau} dx^3\right] \qquad \left(\rho_o = 1\right) \qquad (40)$$

Since P_c cannot be computed exactly, $D^{t+2\tau}$ and D^{t} must differ from the rigid-lid depth D_f. In the order of computation, D^{t} will have been determined by previous computations, but the value of $D^{t+2\tau}$ can still be specified. In practice, $D^{t+2\tau}$ is set equal to D_f in equation (40). Substituting equations (38) and (39) into equation (40) yields

$$\frac{D_f - D^{t}}{(2\tau)^2} + \frac{1}{2\tau}\frac{1}{\sqrt{A}}\frac{\partial}{\partial x^{\alpha}}\left[\frac{\sqrt{A}}{\sqrt{g_{\alpha\alpha}}}\int_{0}^{X^3}\left(\zeta^{t+\tau}\tilde{U}_{\alpha}\right) dx^3\right] = \frac{1}{\sqrt{A}}\frac{\partial}{\partial x^{\alpha}}\left(\frac{\sqrt{A}\,D_f}{g_{\alpha\alpha}}\frac{\partial P_c}{\partial x^{\alpha}}\right) \qquad (41)$$

One can obtain equations for the surface pressure along open inflow and closed lateral boundaries from equation (41). This is done by applying the fictitious boundary conditions given in appendix B as equation (B6) for closed boundaries or equations (B12) and (B13) for inflow boundaries. Equation (41) can be solved for P_c by relaxation when the boundary conditions for P_c are known.

In the derivation of equation (41), no account was taken of the possibility that F_{α} in equations (24) and (25) might contain $U_{\alpha}{}^{t+\tau}$, as would occur when the Coriolis term is integrated implicitly. Consequently, equation (41) can be solved in a straightforward manner only when an explicit integration technique is used. In ocean circulation problems, when long time steps are achieved by filtering external gravity waves, the minimum upper bound for the time increment is determined by the Coriolis term ($f\tau \leq 1$). Since implicit treatment of the Coriolis term increases the allowable time step, a simplistic technique has been devised for implicit integration of the Coriolis term in conjunction with the surface pressure constraint technique for steady-state solutions. Equations (24) and (25) are rewritten to include values of P_c from the previous step, so that

$$\frac{\partial}{\partial t}\left(\zeta U_{\alpha}\right) = -\frac{\sqrt{g_{33}}}{\sqrt{g_{\alpha\alpha}}}\frac{\partial\left(\Delta P_c\right)}{\partial x^{\alpha}} + \sqrt{g_{33}}F_{\alpha} - \frac{\sqrt{g_{33}}}{\sqrt{g_{\alpha\alpha}}}\frac{\partial P_c{}^{t-2\tau}}{\partial x^{\alpha}} \qquad (\alpha \text{ not summed}) \quad (42)$$

where $\Delta P_c = P_c{}^{t} - P_c{}^{t-2\tau}$. The first stage of the integration is then defined by the relationship

$$\frac{\left(\zeta^{t+\tau}\tilde{U}_{\alpha}\right) - \left(\zeta U_{\alpha}\right)^{t-\tau}}{2\tau} = \sqrt{g_{33}}F_{\alpha} - \frac{\sqrt{g_{33}}}{\sqrt{g_{\alpha\alpha}}}\frac{\partial P_c{}^{t-2\tau}}{\partial x^{\alpha}} \qquad (\alpha \text{ not summed}) \quad (43)$$

and with the Coriolis force computed as

$$\sigma_{\alpha\beta}\left(2\omega \cos x^1\right)\left(\frac{U_\beta^{t-\tau} + \tilde{U}_\beta}{2}\right)$$

The second integration stage is performed with

$$\frac{\left(\zeta U_\alpha\right)^{t+\tau} - \left(\zeta^{t+\tau}\tilde{U}_\alpha\right)}{2\tau} = -\frac{\sqrt{g_{33}}}{\sqrt{g_{\alpha\alpha}}}\frac{\partial\left(\Delta P_c\right)}{\partial x^\alpha} \tag{44}$$

When $U_\alpha^{t+\tau}$ converges to a steady-state solution, $P_c^{\,t}$ converges to a steady-state value while $\tilde{U}_\alpha$ converges to $U_\alpha^{t+\tau}$. The Coriolis force is thus treated implicitly.

MODEL SIMULATION RESULTS

A computer model based upon the mathematical model described herein was developed on a global 10^o grid, and some preliminary numerical simulations have been performed. Since a 10^o resolution is too coarse to be compared in detail with the real world, only qualitative features of the flow field are discussed.

In particular, a one-layer flat-bottom model was developed with continental geometry and surface wind stress included; salinity and heat transport were not included because of the long time scales required for these quantities to reach quasi-equilibrium conditions. The annual mean wind stress used to drive the flow field is plotted in figure 1 and was obtained from reference 8. The model was started from rest by applying the wind stress and calculations continued until quasi-equilibrium was reached. The resulting flow field is presented in figure 2 with the zero meridian at the left boundary and extending to 360^o at the right boundary. The model simulation area runs from the North Pole at the upper boundary to the South Pole at the lower boundary. The real-world flow field, taken from reference 9, is shown in figure 3. The model flow field contains large gyres in the correct positions and rotating in the proper sense but without realistic detail. The equatorial currents are observed to be weak. The western intensifications are not present except in the North Atlantic, and the west wind drift is observed in the South Pacific. The probable cause for loss of realism in the model flow field is the coarse grid spacing and the single layer for vertical resolution. During the computer experiment, the ocean's depth remained constant to five significant figures; therefore the constraint pressure technique was working properly. From this experiment, it was concluded that the overall approach is valid and ready for further development on a finer scale.

For detailed simulation results, the reader is referred to reference 5 wherein the results of a model of the North Atlantic Ocean on a 2.5^{o} grid for wind-driven surface currents are presented and compared with real-world data.

CONCLUDING REMARKS

A new pseudo-primitive-variable ocean circulation model has been developed along with a surface pressure constraint technique for filtering fast external gravity waves. The coordinate system follows the ocean bottom and surface. The advantages of the mathematical model presented herein are (1) the ease of determination of boundary conditions, (2) the ability to either resolve or filter external gravity waves, and (3) the ability to utilize coastal bottom topography. The model has been tested under some simple situations which indicate that the surface pressure constraint method can produce divergence-free flow fields in circulation problems involving wind stress. The results of the present report indicate that the new ocean model warrants further investigation.

Langley Research Center
National Aeronautics and Space Administration
Hampton, VA 23665
July 15, 1976

APPENDIX A

SPECIFICATION OF BOUNDARY CONDITIONS FOR COMPUTATION OF RIGID-LID CONSTRAINT PRESSURE

Huw C. Davies
University of Reading
Berkshire, England

In this appendix an idealized analysis is made of the specification of boundary conditions for the constraint pressure field. The approach is similar to, but simpler than, the technique used by Davies in reference 7 to specify boundary conditions for the shallow water equations.

The analysis begins with the equation of motion for a constant-density fluid confined between two parallel plates with a uniform separation distance and bounded by inflow, outflow, and no-flow surfaces. The constraint pressure gradient and the Coriolis force are taken to be the sole driving forces; thus, equations (5) and (6) simplify in rectangular Cartesian coordinates to

$$\frac{\partial U_\alpha}{\partial t} + \frac{\partial}{\partial z^\beta}\left(U_\beta U_\alpha\right) = -\frac{\partial P_c}{\partial z^\alpha} + f\sigma_{\alpha\beta}U_\beta \tag{A1}$$

where

$$\left[\sigma_{\alpha\beta}\right] = \begin{bmatrix} 0 & 1 \\ -1 & 0 \end{bmatrix}$$

The method of solution is to find the rate of growth for perturbations of U_α and then to specify P_c so that perturbations in U_α are minimized. Let perturbations in U_α and P_c be ϵ_α and q, respectively; thus, equation (A1) becomes

$$\frac{\partial}{\partial t}\left(U_\alpha + \epsilon_\alpha\right) + \frac{\partial}{\partial z^\beta}\left[\left(U_\beta + \epsilon_\beta\right)\left(U_\alpha + \epsilon_\alpha\right)\right] = -\frac{\partial}{\partial z^\alpha}\left(P_c + q\right) + f\sigma_{\alpha\beta}\left(U_\beta + \epsilon_\beta\right) \tag{A2}$$

Upon neglecting quadratic perturbation terms and using equation (A1), the governing equation for ϵ_α becomes

$$\frac{\partial \epsilon_\alpha}{\partial t} + \frac{\partial}{\partial z^\beta}\left(U_\beta \epsilon_\alpha + \epsilon_\beta U_\alpha\right) = -\frac{\partial q}{\partial z^\alpha} + f\sigma_{\alpha\beta}\epsilon_\beta \tag{A3}$$

Next, a specification of q is sought which causes the volume integral of $\epsilon_\alpha \epsilon_\alpha$ to decrease in time and thus minimize the total perturbation energy. An equation for $\epsilon_\alpha \epsilon_\alpha$ is found by multiplying equation (A3) by ϵ_α to get

$$\frac{\partial}{\partial t}\left(\frac{\epsilon_\alpha \epsilon_\alpha}{2}\right) + \epsilon_\alpha \frac{\partial}{\partial z^\beta}\left(U_\beta \epsilon_\alpha + \epsilon_\beta U_\alpha\right) = -\epsilon_\alpha \frac{\partial q}{\partial z^\alpha} \tag{A4}$$

The Coriolis force cancels in the summation. Then the time derivative of $\epsilon_\alpha \epsilon_\alpha$ is integrated over a volume ν to yield

$$\frac{\partial}{\partial t}\int_\nu \left(\frac{\epsilon_\alpha \epsilon_\alpha}{2}\right) d\nu = -\int_\nu \epsilon_\alpha \frac{\partial}{\partial z^\beta}\left(U_\beta \epsilon_\alpha\right) d\nu - \int_\nu \epsilon_\alpha \frac{\partial}{\partial z^\beta}\left(\epsilon_\beta U_\alpha\right) d\nu$$

$$- \int_\nu \epsilon_\alpha \frac{\partial q}{\partial z^\alpha} d\nu \tag{A5}$$

In order to analyze the effects of boundary conditions on the left side of equation (A5), the first and last terms on the right side can be rearranged to get

$$\frac{\partial}{\partial t}\int_\nu \left(\frac{\epsilon_\alpha \epsilon_\alpha}{2}\right) d\nu = -\int_\nu \frac{\partial}{\partial z^\beta}\left(U_\beta \epsilon_\alpha \epsilon_\alpha\right) d\nu + \int_\nu U_\beta \frac{\partial}{\partial z^\beta}\left(\frac{\epsilon_\alpha \epsilon_\alpha}{2}\right) d\nu$$

$$- \int_\nu \epsilon_\alpha \frac{\partial}{\partial z^\beta}\left(\epsilon_\beta U_\alpha\right) d\nu - \int_\nu \frac{\partial}{\partial z^\alpha}\left(\epsilon_\alpha q\right) d\nu + \int_\nu q \frac{\partial \epsilon_\alpha}{\partial z^\alpha} d\nu \tag{A6}$$

Consider the right side of equation (A6), wherein

$$\frac{\partial U_\beta}{\partial z^\beta} = \frac{\partial \epsilon_\beta}{\partial z^\beta} = 0$$

The first two integrals combine to give

$$-\int_\nu \frac{\partial}{\partial z^\beta}\left(U_\beta \frac{\epsilon_\alpha \epsilon_\alpha}{2}\right) d\nu$$

the third integral simplifies to

$$-\int_{\nu} \epsilon_{\alpha}\epsilon_{\beta}\frac{\partial U_{\alpha}}{\partial z^{\beta}}\,d\nu$$

and the last term vanishes leaving equation (A6) as

$$\frac{\partial}{\partial t}\int_{\nu}\frac{\epsilon_{\alpha}\epsilon_{\alpha}}{2}\,d\nu = -\int_{\nu}\frac{\partial}{\partial z^{\beta}}\left(U_{\beta}\frac{\epsilon_{\alpha}\epsilon_{\alpha}}{2}\right)d\nu - \int_{\nu}\epsilon_{\alpha}\epsilon_{\beta}\frac{\partial U_{\alpha}}{\partial z^{\beta}}\,d\nu$$

$$-\int_{\nu}\frac{\partial}{\partial z^{\alpha}}\left(\epsilon_{\alpha}q\right)\,d\nu \qquad \text{(A7)}$$

Next, suppose that initially $\epsilon_{\alpha}\epsilon_{\alpha}$ vanishes everywhere on the interior of ν. Then only two surface integrals remain on the right side of equation (A7), those being

$$-\int_{A}\left(U_{\beta}\frac{\epsilon_{\alpha}\epsilon_{\alpha}}{2}\right)n_{\beta}\,dA \quad \text{and} \quad -\int_{A}\left(\epsilon_{\alpha}q\right)n_{\alpha}\,dA$$

where n_{β} is positive outward on surface dA of ν. Consequently, equation (A7) simplifies to

$$\frac{\partial}{\partial t}\int_{\nu}\frac{\epsilon_{\alpha}\epsilon_{\alpha}}{2}\,d\nu = \int_{A_I}\left|\left(U_{\beta}\frac{\epsilon_{\alpha}\epsilon_{\alpha}}{2}n_{\beta}\right)\right|dA_I$$

$$-\int_{A_O}\left|\left(U_{\beta}\frac{\epsilon_{\alpha}\epsilon_{\alpha}}{2}\right)n_{\beta}\right|dA_O - \int_{A_I}\epsilon_{\alpha}qn_{\alpha}\,dA_I$$

$$-\int_{A_O}\epsilon_{\alpha}qn_{\alpha}\,dA_O - \int_{A_C}\epsilon_{\alpha}qn_{\alpha}\,dA_C \qquad \text{(A8)}$$

where dA_I, dA_O, and dA_C refer to inflow, outflow, and closed boundaries, respectively. Since the first term on the right side of equation (A8) increases the perturbation energy, $\epsilon_{\alpha}\epsilon_{\alpha}/2 = 0$ must be maintained on inflow boundaries to insure a stable computation. The second term tends to decrease perturbation energy so that $\epsilon_{\alpha}\epsilon_{\alpha}/2$ may be nonzero on outflow boundaries. Since $\epsilon_{\alpha}\epsilon_{\alpha}/2$ must vanish on inflow boundaries, the third term vanishes, as well as $\epsilon_{\alpha}n_{\alpha}$ on closed boundaries. Thus, equation (A8) reduces to

APPENDIX A

$$\frac{\partial}{\partial t}\int_{\nu}\frac{\epsilon_\alpha\epsilon_\alpha}{2}\,d\nu \leqq -\int_{A_O}\epsilon_\alpha q n_\alpha\,dA_O \tag{A9}$$

The vanishing of $\epsilon_\alpha\epsilon_\alpha$ on inflow boundaries is equivalent to specifying U_α on inflow boundaries. Because of equation (A9), $\epsilon_\alpha n_\alpha q$ vanishes along outflow boundaries; therefore, either $U_\alpha n_\alpha$ or P_c must be specified along the outflow boundary.

APPENDIX B

SPECIAL FORMS OF THE POISSON EQUATION FOR CONSTRAINT PRESSURE ALONG LATERAL BOUNDARIES

The central difference approximation of the governing equation for the constraint pressure, equation (41), takes on a symmetrical form in the problem region interior. Near real and open lateral boundaries, this equation loses its symmetry and assumes special forms which are studied in this appendix.

Equation (41), the governing relation for P_c, is

$$\frac{D_f - D^t}{4\tau^2} + \frac{1}{2\tau}\frac{1}{\sqrt{A}}\frac{\partial}{\partial x^\alpha}\left[\frac{\sqrt{A}}{\sqrt{g_{\alpha\alpha}}}\int_0^{x^3}\left(\zeta^{t+\tau}\tilde{U}_\alpha\right)dx^3\right] = \frac{1}{\sqrt{A}}\frac{\partial}{\partial x^\alpha}\left(\frac{\sqrt{A}}{g_{\alpha\alpha}}D_f\frac{\partial P_c}{\partial x^\alpha}\right) \tag{B1}$$

Consider the staggered time grid lattice with U_1 directed along positive dx^1, U_2 directed along positive dx^2, and $x^1 = I\,\Delta x^1$ and $x^2 = J\,\Delta x^2$ as shown in sketch (a).

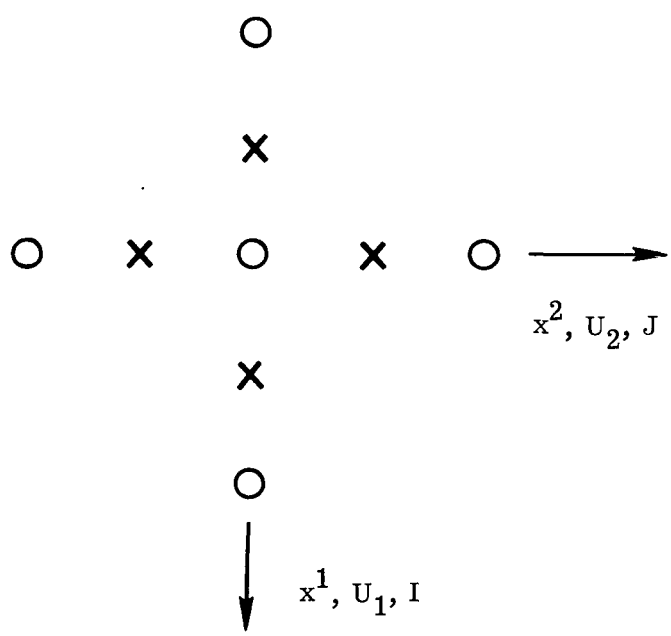

Sketch (a)

The values of ζ, U_1, and U_2 are known at time t on the circles, and the values of ζ, $\tilde{U}_1$, and $\tilde{U}_2$ at time $t + \tau$ are known on the crosses. From equation (B1) the values of P_c at time t are sought on the circles.

APPENDIX B

Interior Solutions

When all the grid points are inside lateral boundaries, the finite-difference approximation for equation (B1) (for simplicity only one vertical layer is considered and $\sqrt{A} = \sqrt{g_{11}} = \sqrt{g_{22}} = 1$) is

$$\frac{D_f(I,J) - D^t(I,J)}{4\tau^2} + \frac{\Delta x^3}{2\tau}\left[\frac{\zeta^{t+\tau}(I+1,J)\,\tilde{U}_1(I+1,J) - \zeta^{t+\tau}(I-1,J)\,\tilde{U}_1(I-1,J)}{2\,\Delta x^1}\right]$$

$$+ \frac{\Delta x^3}{2\tau}\left[\frac{\zeta^{t+\tau}(I,J+1)\,\tilde{U}_2(I,J+1) - \zeta^{t+\tau}(I,J-1)\,\tilde{U}_2(I,J-1)}{2\,\Delta x^2}\right]$$

$$= \frac{D_f(I+1,J)}{2\,\Delta x^1}\left[\frac{P_c(I+2,J) - P_c(I,J)}{2\,\Delta x^1}\right] - \frac{D_f(I-1,J)}{2\,\Delta x^1}\left[\frac{P_c(I,J) - P_c(I-2,J)}{2\,\Delta x^1}\right]$$

$$+ \frac{D_f(I,J+1)}{2\,\Delta x^2}\left[\frac{P_c(I,J+2) - P_c(I,J)}{2\,\Delta x^2}\right] - \frac{D_f(I,J-1)}{2\,\Delta x^2}\left[\frac{P_c(I,J) - P_c(I,J-2)}{2\,\Delta x^2}\right] \qquad \text{(B2)}$$

Closed Lateral Boundaries

In order to describe the treatment of computations near closed lateral boundaries, the boundary parallel to dx^2 is used as an example. The computations at other boundaries are treated similarly. Assume that the zero depth point associated with a closed lateral boundary occurs at I - 2 (see sketch (a)). Then the boundary is parallel to dx^2 at I - 1, and to prevent mass loss from the system, $U^{t+\tau}(I-1,J)$ must vanish. For the single layer being considered and with $\sqrt{A} = \sqrt{g_{11}} = \sqrt{g_{22}} = 1$, equation (38) integrated over the depth gives

$$\frac{\Delta x^3}{2\tau}\left[\left(\zeta U_1\right)^{t+\tau} - \left(\zeta^{t+\tau}\tilde{U}_1\right)\right] = -D_f \frac{\partial P_c}{\partial x^1} \qquad \text{(B3)}$$

The finite-difference notation is (since $U_1{}^{t+\tau}(I-1,J) = 0$)

$$\frac{\Delta x^3}{2\tau}\zeta^{t+\tau}(I-1,J)\,\tilde{U}_1(I-1,J) = \frac{1}{2\,\Delta x^1} D_f(I-1,J)\left[P_c(I,J) - P_c(I-2,J)\right] \qquad \text{(B4)}$$

APPENDIX B

When equation (B4) is substituted into equation (B2), the terms involving $\tilde{U}_1(I-1,J)$ and $P_c(I,J) - P_c(I-2,J)$ cancel leaving

$$\frac{D_f(I,J) - D^t(I,J)}{4\tau^2} + \frac{\Delta x^3}{2\tau}\left[\frac{\zeta^{t+\tau}(I+1,J)\ \tilde{U}_1(I+1,J)}{2\ \Delta x^1}\right]$$

$$= \frac{D_f(I+1,J)}{2\ \Delta x^1}\left[\frac{P_c(I+2,J) - P_c(I,J)}{2\ \Delta x^1}\right] - \frac{\Delta x^3}{2\tau}\left[\frac{\zeta^{t+\tau}(I,J+1)\ \tilde{U}_2(I,J+1) - \zeta^{t+\tau}(I,J-1)\ \tilde{U}_2(I,J-1)}{2\ \Delta x^2}\right]$$

$$+ \frac{D_f(I,J+1)}{2\ \Delta x^2}\left[\frac{P_c(I,J+2) - P_c(I,J)}{2\ \Delta x^2}\right] - \frac{D_f(I,J-1)}{2\ \Delta x^2}\left[\frac{P_c(I,J) - P_c(I,J-2)}{2\ \Delta x^2}\right] \qquad \text{(B5)}$$

which does not involve $\tilde{U}_1(I-1,J)$ or $P_c(I-2,J)$. As an alternative to using equation (B5), one can use equation (B2) for the case under consideration by applying the fictitious boundary conditions

$$\left.\begin{aligned}\tilde{U}_1(I-1,J) &= 0\\ P_c(I-2,J) &= P_c(I,J)\end{aligned}\right\} \qquad \text{(B6)}$$

Inflow Boundaries

To describe boundary computations for inflow boundaries, a boundary passing through the grid point (I-1,J) parallel to dx^2 is used as an example. The development of an equation for the computation of P_c follows the development of equation (41) in the text. Consider a finite-difference approximation for equation (40) (for one layer and $\sqrt{A} = \sqrt{g_{11}} = \sqrt{g_{22}} = 1$) which contains both boundary values and interior values of U_α

$$\frac{D_f(I,J) - D^t(I,J)}{2\tau} = -\Delta x^3\left[\frac{\zeta^{t+\tau}(I+1,J)\ U_1{}^{t+\tau}(I+1,J) - \zeta^{t+\tau}(I-1,J)\ U_1{}^{t+\tau}(I-1,J)}{2\ \Delta x^1}\right]$$

$$- \Delta x^3\left[\frac{\zeta^{t+\tau}(I,J+1)\ U_2{}^{t+\tau}(I,J+1) - \zeta^{t+\tau}(I,J-1)\ U_2{}^{t+\tau}(I,J-1)}{2\ \Delta x^2}\right] \qquad \text{(B7)}$$

APPENDIX B

In the case under consideration, $U_1^{t+\tau}(I-1,J)$ is a boundary value which, according to appendix A, must be prescribed. The other three velocities involved in equation (B7) are $U_1^{t+\tau}(I+1,J)$, $U_2^{t+\tau}(I,J+1)$, and $U_2^{t+\tau}(I,J-1)$. Each of these velocities must be computed from either equation (38) or else equation (39). Recalling again the simplification used (one layer and $\sqrt{A} = \sqrt{g_{11}} = \sqrt{g_{22}} = 1$), one has for $U_1^{t+\tau}(I+1,J)$ from equation (38)

$$\frac{\Delta x^3}{2\tau}\,\zeta^{t+\tau}(I+1,J)\,U_1^{t+\tau}(I+1,J) = \frac{\Delta x^3}{2\tau}\,\zeta^{t+\tau}(I+1,J)\,\tilde{U}_1(I+1,J) - \frac{D_f(I+1,J)}{2\,\Delta x^1}\left[P_c(I+2,J) - P_c(I,J)\right] \tag{B8}$$

for $U_2^{t+\tau}(I,J+1)$ from equation (39)

$$\frac{\Delta x^3}{2\tau}\,\zeta^{t+\tau}(I,J+1)\,U_2^{t+\tau}(I,J+1) = \frac{\Delta x^3}{2\tau}\,\zeta^{t+\tau}(I,J+1)\,\tilde{U}_2(I,J+1) - \frac{D_f(I,J+1)}{2\,\Delta x^2}\left[P_c(I,J+2) - P_c(I,J)\right] \tag{B9}$$

and for $U_2^{t+\tau}(I,J-1)$

$$\frac{\Delta x^3}{2\tau}\,\zeta^{t+\tau}(I,J-1)\,U_2^{t+\tau}(I,J-1) = \frac{\Delta x^3}{2\tau}\,\zeta^{t+\tau}(I,J-1)\,\tilde{U}_2(I,J-1) - \frac{D_f(I,J-1)}{2\,\Delta x^2}\left[P_c(I,J) - P_c(I,J-2)\right] \tag{B10}$$

Next, the governing equation for P_c for the case under consideration is obtained by substituting equations (B8), (B9), and (B10) into equation (B7) to get

$$\frac{D_f(I,J) - D^t(I,J)}{4\tau^2} + \frac{\Delta x^3}{2\tau}\left[\frac{\zeta^{t+\tau}(I+1,J)\,\tilde{U}_1(I+1,J) - \zeta^{t+\tau}(I-1,J)\,U_1^{t+\tau}(I-1,J)}{2\,\Delta x^1}\right]$$

$$+ \frac{\Delta x^3}{2\tau}\left[\frac{\zeta^{t+\tau}(I,J+1)\,\tilde{U}_2(I,J+1) - \zeta^{t+\tau}(I,J-1)\,\tilde{U}_2(I,J-1)}{2\,\Delta x^2}\right]$$

$$= \frac{D_f(I+1,J)}{2\,\Delta x^1}\left[\frac{P_c(I+2,J) - P_c(I,J)}{2\,\Delta x^1}\right] + \frac{D_f(I,J+1)}{2\,\Delta x^2}\left[\frac{P_c(I,J+2) - P_c(I,J)}{2\,\Delta x^2}\right]$$

$$- \frac{D_f(I,J-1)}{2\,\Delta x^2}\left[\frac{P_c(I,J) - P_c(I,J-2)}{2\,\Delta x^2}\right] \tag{B11}$$

Equation (B11) is the proper form of equation (41) to use adjacent to inflow boundaries. Here again one can make equation (B2) equal to equation (B11) by specifying

$$\tilde{U}_1(I-1,J) = U_1^{t+\tau}(I-1,J) \tag{B12}$$

along with

$$P_c(I-2,J) = P_c(I,J) \tag{B13}$$

as a fictitious boundary condition on P_c. Thereby the symmetry of equation (B2) is preserved.

Outflow Boundaries

The constraint pressure is usually specified along outflow boundaries. Velocity boundary conditions are then specified by upstream differencing.

REFERENCES

1. Manabe, Syukuro; and Bryan, Kirk: Climate and the Ocean Circulation. Mon. Weather Rev., vol. 97, no. 11, Nov. 1969, pp. 739-827.

2. Leendertse, Jan J.; and Liu, Shiao-Kung: A Three-Dimensional Model for Estuaries and Coastal Seas: Volume II, Aspects of Computation. R-1764-OWRT, RAND Corp., June 1975. (Available from NTIS as PB 244 501.)

3. Veziroglu, T. Nejat; and Lee, Samuel S.: Application of Remote Sensing for Prediction and Detection of Thermal Pollution. NASA CR-139182, 1974.

4. Avis, Lee M.; Turner, Richard E.; and Rees, Thomas H.: A Generalized Tensor Formulation of Atmosphere and Seas Dynamics. NASA TR R-441, 1975.

5. Rees, Thomas H.; and Turner, Richard E.: Calculation of Wind-Driven Surface Currents in the North Atlantic Ocean. NASA TN D-8223, 1976.

6. Oliger, J. E.; Wellck, R. E.; Kasahara, A.; and Washington, W. M.: Description of NCAR Global Circulation Model. NCAR-TN/STR-56, May 1970. (Reprinted Mar. 1971.)

7. Davies, Huw C.: On the Lateral Boundary Conditions for the Primitive Equations. J. Atmos. Sci., vol. 30, no. 1, Jan. 1973, pp. 147-150.

8. Hellerman, S.: An Updated Estimate of the Wind Stress on the World Ocean. Mon. Weather Rev., vol. 95, no. 9, Sept. 1967, pp. 607-626. (Corrected in vol. 96, no. 1, Jan. 1968, pp. 63-74.)

9. Gross, M. Grant: Oceanography – A View of the Earth. Prentice-Hall, Inc., c.1972, p. 214.

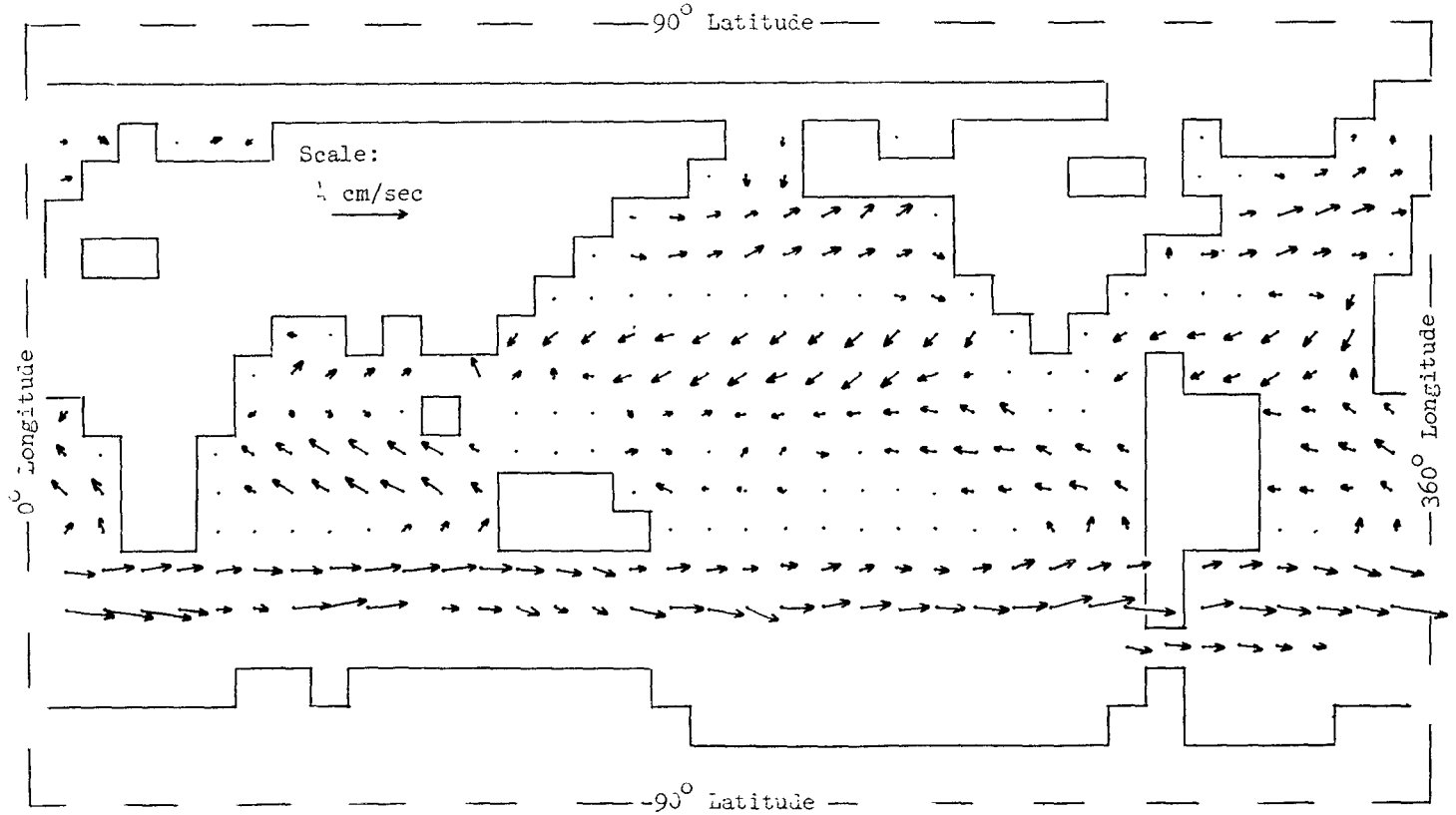

Figure 1.- Annual mean wind stress on global oceans (ref. 8).

Figure 2.- Current vector field from model in quasi-equilibrium. 10 days from initiation. One (two) bars across arrow denote two (four) times scale.

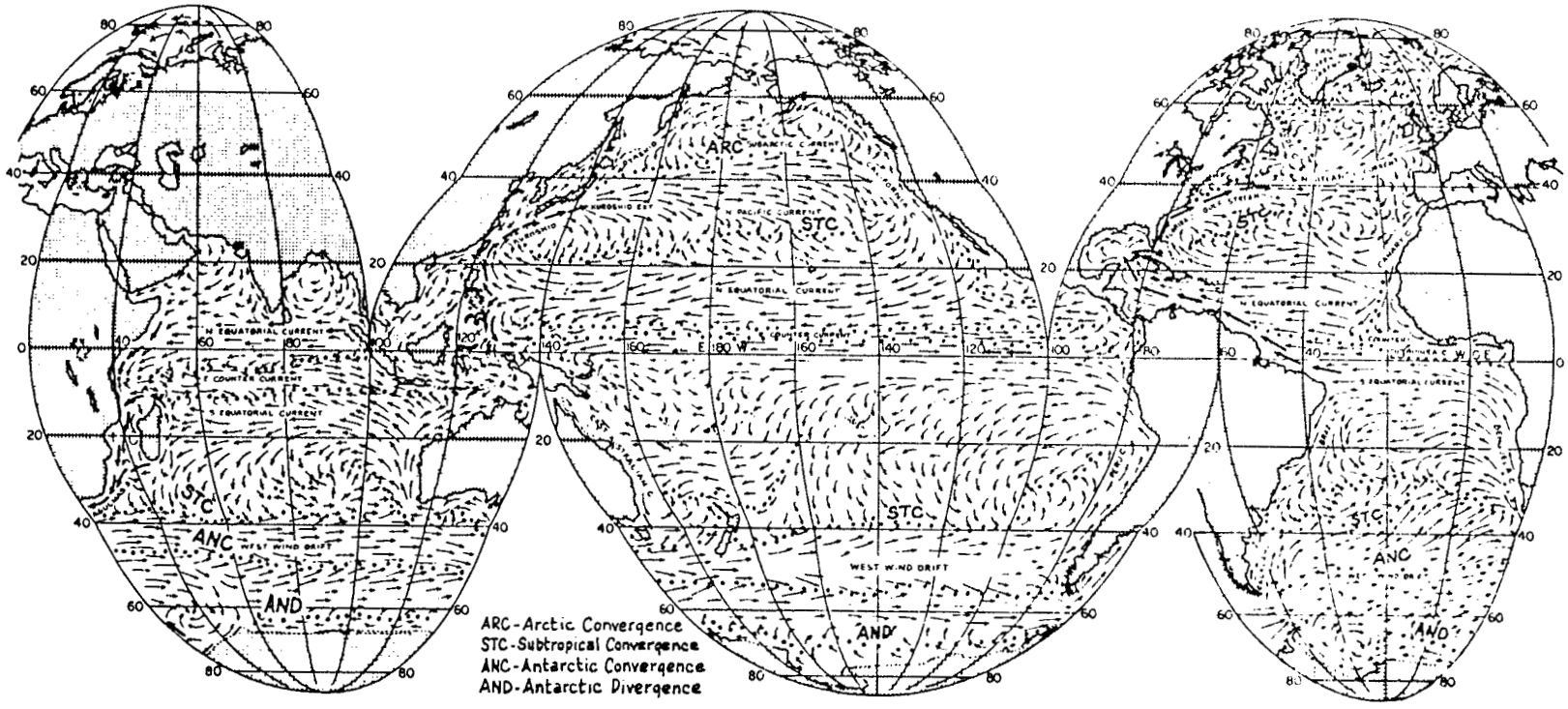

Figure 3.- Observed global currents. (Reproduced from ref. 9 by permission of publisher.)

"The aeronautical and space activities of the United States shall be conducted so as to contribute . . . to the expansion of human knowledge of phenomena in the atmosphere and space. The Administration shall provide for the widest practicable and appropriate dissemination of information concerning its activities and the results thereof."

—NATIONAL AERONAUTICS AND SPACE ACT OF 1958

NASA SCIENTIFIC AND TECHNICAL PUBLICATIONS

TECHNICAL REPORTS: Scientific and technical information considered important, complete, and a lasting contribution to existing knowledge.

TECHNICAL NOTES: Information less broad in scope but nevertheless of importance as a contribution to existing knowledge.

TECHNICAL MEMORANDUMS: Information receiving limited distribution because of preliminary data, security classification, or other reasons. Also includes conference proceedings with either limited or unlimited distribution.

CONTRACTOR REPORTS: Scientific and technical information generated under a NASA contract or grant and considered an important contribution to existing knowledge.

TECHNICAL TRANSLATIONS: Information published in a foreign language considered to merit NASA distribution in English.

SPECIAL PUBLICATIONS: Information derived from or of value to NASA activities. Publications include final reports of major projects, monographs, data compilations, handbooks, sourcebooks, and special bibliographies.

TECHNOLOGY UTILIZATION PUBLICATIONS: Information on technology used by NASA that may be of particular interest in commercial and other non-aerospace applications. Publications include Tech Briefs, Technology Utilization Reports and Technology Surveys.

Details on the availability of these publications may be obtained from:

SCIENTIFIC AND TECHNICAL INFORMATION OFFICE

NATIONAL AERONAUTICS AND SPACE ADMINISTRATION

Washington, D.C. 20546